Drive-by damage detection with a TSD and time-shifted curvature

Jennifer C. Keenahan*[1],
Eugene J. OBrien[1]

[1]*School of Civil Engineering, University College Dublin, Belfield, Dublin 4, Ireland*

Abstract. 'Drive-by' damage detection is the concept of using sensors on a passing vehicle to detect damage in a bridge. The newly developed Traffic Speed Deflectometer (TSD) is a device used for pavement velocity/deflection measurements and is investigated here in numerical simulations as a means of bridge damage detection. A TSD vehicle model containing five displacement sensors is simulated crossing a simply supported finite element beam containing damage simulated as a loss in stiffness of one of the elements. Time-shifted curvature is derived from the displacements and is proposed as a novel damage indicator, which removes the influence of the road profile and all vehicle motions except for pitch. Results show that the time-shifted curvature can be reliably used as a damage indicator in the presence of noise and changes in transverse position of the vehicle on the bridge.

Keywords: bridge; damage; traffic speed deflectometer; curvature; kurtosis; drive-by; SHM, health monitoring

1. Introduction

There has been a move towards sensor based monitoring of bridge condition in recent years owing to the shortcomings of visual inspections, combined with the increase in computational power and signal processing capacity. A further advantage of direct instrumentation of bridges is the permanent monitoring of long term processes. More recently, a small number of authors have shifted to the instrumentation of a passing vehicle, rather than the bridge, in order to assess bridge condition. This approach is referred to as 'drive-by' bridge inspection (Kim & Kawatani, 2009). Assessments of this nature do not require lane closures, thus reducing traffic delays and traffic management costs and improving levels of safety. Further, bridges do not need to be instrumented, so the concept has the potential to be far more cost effective than Structural Health Monitoring.

Yang et al. (2004) theoretically verify the drive-by concept by detecting bridge frequencies from the dynamic response of an instrumented vehicle traversing a bridge in computer simulations. The vehicle is modelled as a sprung mass and the bridge as a simply supported beam. The bridge frequency is contained in and is extracted from the vertical vehicle acceleration spectrum. However this research does not allow for the pitching and rolling motions of a real vehicle, damping and suspension mechanisms in the vehicle and pavement roughness.

Lin and Yang (2005) conduct field trials to examine the drive-by concept. A single-degree-of-freedom sprung mass trailer, towed by a four wheel truck, is used to scan the fundamental frequency of vibration of the Da-Wu-Lun Bridge, near the northern coast of Taiwan. The vertical acceleration response of the trailer is processed by a Fast Fourier Transform (FFT) to extract the frequencies of

*Corresponding author, Ph.D., E-mail: jennifer.keenahan@ucd.ie

vibration of the bridge. For speeds less than 40 km h^{-1} on good road profiles, the bridge frequency is identified. However, as the vehicle speed increases the bridge frequency becomes difficult to detect, which is attributed to the interaction with the road profile. Oshima et al. (2008) also experimentally evaluate a method of extracting the frequencies of a bridge from the responses of a passing vehicle. Accelerometers are installed on each of the wheels of an ordinary passenger vehicle that traverses a steel bridge with four main girders. The bridge frequency, determined from the vehicle response, shows good agreement with the frequency directly monitored on the bridge.

Yang and Chang (2009) further advance the concept of drive-by bridge inspections by proposing a method of examining bridge frequencies of higher modes. The method first processes the vehicle response by Empirical Mode Decomposition to generate intrinsic mode functions, and then the FFT is applied. Both theoretical and experimental investigations show that the bridge frequencies of higher modes are detected using this approach. However, the necessity for at least three runs of the tractor-trailer traversing the bridge in field trials, under exactly the same conditions, is an obvious drawback.

McGetrick et al. (2009) investigate the effect of a road profile on the feasibility of using an instrumented quarter-car in numerical simulations to detect bridge natural frequencies. Results indicate that the approach works well in the absence of a road profile. However, when an ISO Class 'A' (ISO 8608, 1995) road profile is included in simulations, the bridge frequencies are only detected for speeds of up to 5 m s^{-1}. The inclusion of road surface roughness in numerical simulations excites the vehicle to greater amplitudes than that of the bridge and poses challenges in identifying bridge frequencies (González et al., 2012).

The use of drive-by methods for bridge health monitoring, rather than bridge frequency detection has been initiated by Kim and Kawatani (2009), McGetrick et al. (2010a), McGetrick et al (2010b) and Toshinami et al. (2010). In laboratory experiments, Kim and Kawatani (2009) assess the feasibility of drive-by inspections for damage detection in short span bridges. A scale bridge model is adopted as a girder with a road surface profile and the vehicle model allows for vertical axle motions. The girder is cut in three locations to one third of the beam depth. Damage location and severity are successfully estimated. Later, Toshnami et al. (2010) numerically investigate the feasibility of detecting the frequency of a 40 m bridge span, idealised as a series of beam elements, from the vibration of a vehicle, idealised as a two degree-of-freedom system allowing for bounce and pitch motions during a drive-by inspection. Damage is simulated as a 50% reduction in the bending stiffness of ten of the beam elements and the bridge frequency appears in the vehicle's vibration response. More recently, Yabe and Miyamoto (2012) use the mean displacement of the rear axle of a city bus passing over a bridge a large number of times as a damage indicator.

Cerda et al. (2012) use a scale model of a moving vehicle traversing a simply supported beam to experimentally validate the drive-by concept, where changes in the condition of the bridge are simulated by the addition of mass to the mid-span. Vertical acceleration signals from the vehicle are processed using the Short-Time Fourier Transform and results suggest that there is a linearly increasing trend between the number of runs and the quality of frequency detection, and that lower vehicle speeds are better for identifying changes in the natural frequency of the bridge.

While the move to using drive-by methods for damage detection seems successful, shortcomings include the exclusion of axle-hop degrees-of-freedom from the vehicle model, the need for the vehicle to travel at moderate speeds (González et al., 2008; McGetrick et al., 2013), and that small levels of damage cannot be easily detected. Unlike much of the previous work in this area, Keenahan et al. (2014) investigate the possibilities of the vehicle model traversing the bridge at full highway speeds. In numerical simulations, accelerometers are fitted to a truck-trailer vehicle system for

bridge monitoring, where damage in the bridge is simulated as changes in bridge damping. Results show that the bridge frequency and changes in damping are detected and are of similar quality to results obtained from an accelerometer located on the bridge. At a similar time, Yang et al. (2012) propose using two connected vehicles of identical mass and stiffness to remove the dominating effect of the road profile. The vehicles move at constant speed across the bridge, the acceleration responses are recorded and are then converted to frequency spectra. The spectrum for one vehicle is subtracted from the other and a residual spectrum is found, for which the road surface roughness is effectively removed and the bridge frequency is readily detected.

More recently, McGetrick et al. (2017) has harnessed the potential of smartphone technology for drive-by monitoring. In this research, the use of low-cost sensors incorporating global navigation satellite systems was investigated for implementation of the drive-by system in practice, via field trials with an instrumented vehicle. It was found that smartphone tracking applications compared favourably in terms of accuracy, cost and ease of use compared to professional devices.

Experimental validation of the drive-by concept was conducted in a laboratory environment by (McGetrick et al., 2015). The vehicle-bridge interaction model consisted of a scaled two-axle vehicle model crossing a simply supported steel beam with a scaled road surface profile. An algorithm for bridge damage detection was validated using the experimental data and the bream stiffness was identified with a reasonable degree of accuracy. Further laboratory experiments were completed by (Kim et al., 2017) who equipped a test vehicle system with accelerometers to verify three drive-by methods: (1) bridge-frequency extraction using the Fourier spectrum of a vehicle's dynamic response, (2) damage detection using the change in a vehicle's spectral distribution pattern, and (3) roadway surface profile identification.

Further validation of the drive-by concept has been conducted in field trials by (Kim et al., 2016) who investigated a continuous steel Gerber-truss bridge with artificial damage applied. It investigated the sensitivities of a number of quantities to bridge damage including the identified modal parameters and their statistical patterns, Nair's damage indicator and its statistical pattern and different sets of measurement points. Decisions on bridge health condition were made and the sensitivity of variables were evaluated.

Much of the research to date in the area of drive-by inspection uses two-axle cars or truck-trailer vehicle models, retrospectively fitted with sensors. The recently developed prototype Rolling Weight Deflectometer (RWD), presented first by Briggs et al. (2000) in the United States, is the first move towards the development of a vehicle model designed specifically for 'drive-by' inspections of road pavements. It is proposed as a replacement for the Falling Weight Deflectometer (FWD) which has several disadvantages; it must stop at each test site for several minutes which limits the productivity of the device, and extreme care must be taken when testing on busy highways. More recently, in 2004, the Transport Research Laboratory (TRL) in the UK identified a similar Danish device, the 'High-speed Deflectograph', later renamed the 'Traffic Speed Deflectometer' (TSD), capable of performing deflection surveys at speeds of up to 80 km h^{-1}, avoiding traffic disruption and expensive traffic management.

The TSD is a collection of non contact lasers mounted at equal spacing on a rigid beam, housed in the trailer of an articulated lorry that directly, continuously and very accurately measures vertical velocities from which deflections are inferred at highway speeds. These deflections have been successfully used as damage indicators in pavement damage detection (Briggs et al., 2000). Performing surveys at highway speeds enables high levels of daily road coverage, reducing costs and potentially allowing a single machine to test a small road network at least once per year. Such surveys would enable the undertaking of trend analysis as well as monitoring seasonal variations in

pavements (Jenkins, 2009).

In numerical vehicle-bridge interaction simulations, this paper is the first to investigate the use of the TSD in a drive-by bridge damage detection context. The purpose of this is to determine whether bridge damage can be detected using the newly developed Traffic Speed Deflectometer, with no other vehicles present on the bridge. Initially, a TSD model with three displacement sensors is proposed for bridge damage detection, which removes the bounce motion of the vehicle and the road profile influence. The TSD model is then developed to consider a vehicle with five displacement sensors and the damage indicator of time-shifted kurtosis is presented as a means of removing the bounce motions, the profile and the pitch motions of the vehicle. The use of curvature has previously been presented as a means to determine a local loss of stiffness in a bridge using the drive-by concept in (OBrien et al., 2017). Five different levels of damage are considered, and the approach also looks at changes in the transverse position of the road profile and the addition of noise. It is anticipated that the numerical models developed in this paper will inform future developments in drive-by bridge damage detection.

2. Dynamic modelling of TSD

The TSD is modelled here as a half-car crossing a simply supported beam with an ISO Class 'A' (ISO 8608, 1995) road profile (Fig. 1). To date, TSD's have been designed to measurement pavement stiffness. The configuration used here (axle spacings and sensor locations) is not intended to reflect current practice but is simplified deliberately to its most basic level. The vehicle-bridge interaction is modelled as a coupled system, the solution is given at each time step and no iteration is required in the computational process.

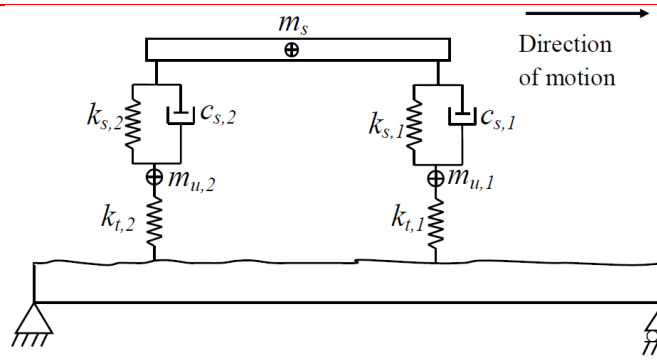

Fig. 1 Half-car model of the TSD

2.1 Bridge model

The bridge is simulated as a 20 m simply supported FE beam model. It consists of 20 discretised beam elements with 4 degrees of freedom. Therefore the beam model has a total of $n = 42$ degrees of freedom. The beam has a modulus of elasticity of $E = 35$ GPa and the density is $\rho = 2446$ kg m^{-3}, values typical of reinforced or prestressed concrete. The second moment of area is taken as $J = 0.3333$ m^4, reflecting a 4 m lane width and a solid section with a span/depth ratio of 20. The bridge damping ratio is 3%. The response of the discretised beam model to moving time-varying forces is

given by the system of equations:

$$M_b\ddot{y}_b + C_b\dot{y}_b + K_b y_b = N_b f_{\text{int}} \quad (1)$$

where M_b, C_b and K_b are the global mass, damping and stiffness matrices of the beam model respectively. The terms $\ddot{y}_b$, $\dot{y}_b$ and y_b are the vectors of nodal bridge accelerations, velocities and displacements respectively. The product, $N_b f_{\text{int}}$, is the vector of forces applied to the bridge nodes. The vector, f_{int}, contains the interaction forces between the vehicle and the bridge and is described by:

$$f_{\text{int}} = P + F_{t,i} \quad (2)$$

where the vector $F_{t,i}$ contains the dynamic wheel contact forces of each axle and P is the static axle load vector. The location matrix, N_b, distributes the applied interaction forces on beam elements to equivalent forces acting on nodes. This location matrix can be used to calculate bridge displacements under each wheel, y_{br}:

$$y_{br} = N_b^T y_b \quad (3)$$

Although complex damping mechanisms may be present in the structure, viscous damping is typically used for bridge structures and is deemed to be sufficient to reproduce the bridge response accurately. Therefore, Rayleigh damping is adopted here to model viscous damping:

$$C_b = \alpha M_b + \beta K_b \quad (4)$$

Where α and β are constants. The damping ratio is assumed to be the same for the first two modes (Yang et al., 2004) and α and β are obtained from $\alpha = 2\xi\omega_1\omega_2/(\omega_1 + \omega_2)$ and $\beta = 2\xi/(\omega_1 + \omega_2)$ where ω_1 and ω_2 are the first two natural frequencies of the bridge (Clough and Penzien, 1975).

2.2 Vehicle model

The vehicle is modelled as a 4 degree-of-freedom half-car travelling at a constant speed of 20 m s^{-1}. It is assumed that a constant velocity can be achieved in practice using cruise control. The four independent degrees of freedom correspond to sprung mass bounce displacement, y_s, sprung mass pitch rotation, θ_s and axle hop displacements of the unsprung masses, $y_{u,1}$ and $y_{u,2}$ at axle 1 and axle 2 respectively. The vehicle body mass is represented by the sprung mass, m_s, and the axle components are represented by unsprung masses, $m_{u,1}$ and $m_{u,2}$. The sprung mass connects to the axle masses via a combination of springs of linear stiffness $k_{s,i}$ and viscous dampers with damping coefficients, $C_{s,i}$ which represent the suspension components for the front and rear axles (i = 1,2). The axle masses then connect to the road surface via springs with linear stiffnesses, $k_{t,i}$ which represent the tyre components for the front and rear axles (i = 1,2). All the property values of the half-car are listed in Table 1 and are based on values gathered from the literature (Cebon, 1999; González, 2010; Harris et al, 2007). While the method is insensitive to changes in these vehicle

properties for a given bridge assessment, it will be necessary to recalibrate the vehicle model properties from year to year to allow for the risk that vehicle aging influences properties and therefore the performance of the algorithm. The geometry is obtained from a manufacturer specification for an 18 tonne two-axle truck (DAF Trucks Limited, 2012).

Table 1 Half-car properties

Property	Symbol	Value	Unit
Body mass	m_s	18 000	kg
Axle masses	$m_{u,1}$, $m_{u,2}$	700	kg
Suspension stiffnesses	$k_{s,1}$, $k_{s,2}$	400 000	N m^{-1}
Suspension damping	$C_{s,1}$, $C_{s,2}$	10 000	Ns m^{-1}
Tyre stiffnesses	$k_{t,1}$, $k_{t,2}$	1.75 x 10^6	N m^{-1}

The equations of motion of the vehicle model are obtained by imposing equilibrium of all forces and moments acting on the vehicle and expressing them in terms of the degrees of freedom. They are given by

$$M_v \ddot{y}_v + C_v \dot{y}_v + K_v y_v = f_v \tag{5}$$

where M_v, C_v and K_v are the mass, damping and stiffness matrices of the vehicle respectively. The vectors, y_v, $\dot{y}_v$ and $\ddot{y}_v$ are the vehicle displacements, their velocities and accelerations respectively. The displacement vector of the vehicle is, $y_v = \{y_s, \theta_s, y_{u,1}, y_{u,2}\}$. The vector f_v contains the time varying interaction forces applied by the vehicle to the bridge: $f_v = \{0 \quad 0 \quad -F_{t,1} \quad -F_{t,2}\}^T$. The term $F_{t,i}$, represents the dynamic interaction force at wheel i:

$$F_{t,i} = k_{t,i}(y_{u,i} - y_{br} - r_i)_v \tag{6}$$

2.3 Road profile generation and filtering

Cebon (1999) describes how an artificial road surface topography can be generated stochastically based on the ISO method (ISO 8608, 1995) of representing road surface roughness with a power spectral density function and then applying the inverse Fast Fourier Transform. (ISO 8608, 1995) define a class 'A' road profile (Fig. 2) and label it a 'very good profile'. This profile is expected in a well maintained highway and is considered in this work. It has a geometric spatial mean of 8 × 10^{-6} m^3 cycle^{-1}. A moving average filter is applied to the generated road profile heights, r_i, over a distance of 0.24 m to simulate the attenuation of short wavelength disturbances by the tyre contact patch (Harris et al., 2007).

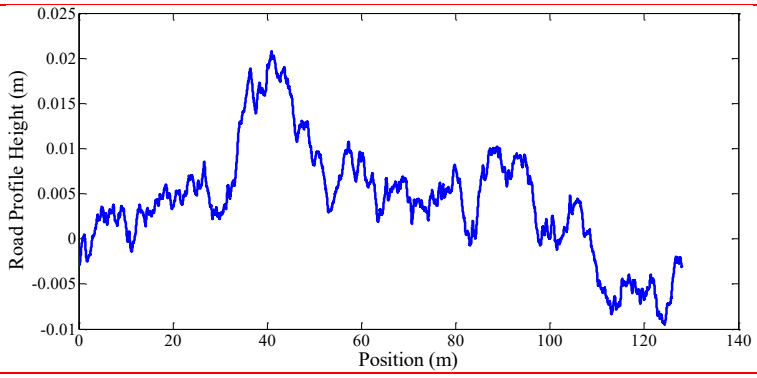

Fig. 2 Road profile

2.4 Coupling of the vehicle-bridge system

The dynamic interaction between the vehicle and the bridge is implemented in Matlab. The vehicle and the bridge are coupled at the tyre contact points via the interaction force vector, f_{int}. Combining Equation (1) and Equation (5), the coupled equation of motion is formed as,

$$M_g\ddot{u} + C_g\dot{u} + K_g u = F \tag{7}$$

where M_g and C_g are the combined system mass and damping matrices respectively, K_g is the coupled time-varying system stiffness matrix and F is the system force vector. The vector, $u = \{y_v, y_{br}\}^T$ is the displacement vector of the system. The equations for the coupled system are solved using the Wilson-Theta integration scheme (Bathe and Wilson, 1976; Tedesco et al, 1999). The optimal value of the parameter $\theta = 1.420815$ is used for unconditional stability in the integration schemes (Weaver and Johnston, 1987). The scanning frequency used for all simulations is 1000 Hz.

3. Modelling the TSD with three sensors

The TSD is modelled as a 4 m long half-car travelling on a 100 m approach length followed by a 20 m simply supported beam, with a Class 'A' road profile as described in Section 2. Three sensors are simulated; one at the front of the vehicle, one in the middle and one at the rear. The centre of gravity of the vehicle is at the geometric centre of the half-car. It is proposed that the sensors read the distance from the vehicle to the ground, plus some combination of the bounce (vertical motion of the vehicle body), pitch (rotation of the vehicle body), road profile height and bridge displacements. The displacements read by each sensor, h_A, h_B and h_C, are given by Equations (8) – (10), where the vehicle height above the ground, *h*, is taken to be 0.5 m. The scanning rate is 1000 Hz.

$$h_A = h - bounce - b * pitch - road_A + bridge_A \tag{8}$$

$$h_B = h - bounce - road_B + bridge_B \tag{9}$$

$$h_C = h - bounce + b^* pitch - road_C + bridge_C \tag{10}$$

at a given instant in time, where $road_A$, $road_B$ and $road_C$ are the road profile heights read by sensors A, B and C respectively, and $bridge_A$, $bridge_B$ and $bridge_C$ are the bridge displacements read by sensors A, B and C respectively. Bridge damage is included in simulations as recommended by Sinha et al. (2002) where a crack causes a loss in stiffness over a region of three times the beam depth varying linearly with a maximum at the centre, in this case, the 14th element out of a total of 20 elements. The TSD is simulated crossing the bridge six times, once for the healthy case and once for each of five different damage levels up to a maximum of 50%. It is acknowledged that this represents a potentially catastrophic level of damage but 10% and 20% cracks are similar to the levels assumed by many authors (González & Hester, 2013; Hester et al., 2008). The displacements read by each sensor can be seen in Fig. 3.

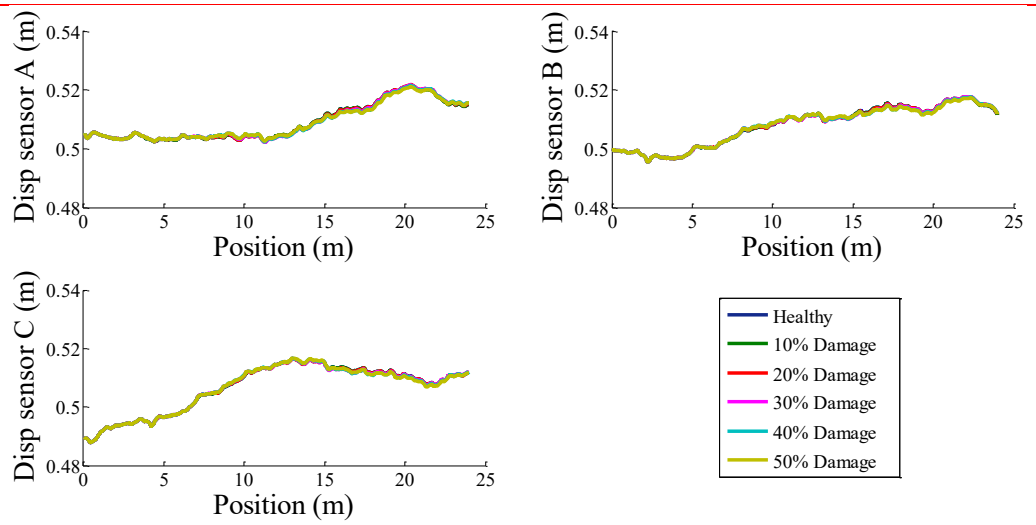

Fig. 3 The displacements read by each of the sensors for different damage levels

Fig. 3 illustrates the displacements read by each of the three sensors at five different damage levels. It is not possible to distinguish between the different damage levels as each of the displacement signals are overlapping one another. For clarity, the individual components of Equations (8) – (10) are now examined to show the contribution of each to the total displacement signals read by each sensor. The contribution of the bounce and pitch motions to the sensor readings can be seen in Fig. 4 and the bridge displacements read by each sensor are shown in Fig. 5. Each sensor reads the same portion of the road profile, but at different times.

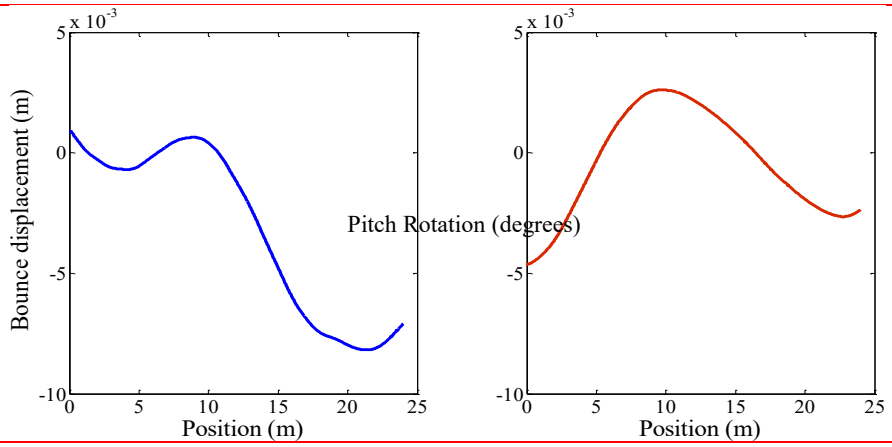

Fig. 4 The portion of the bounce and pitch read by the sensors (identical for all three sensors)

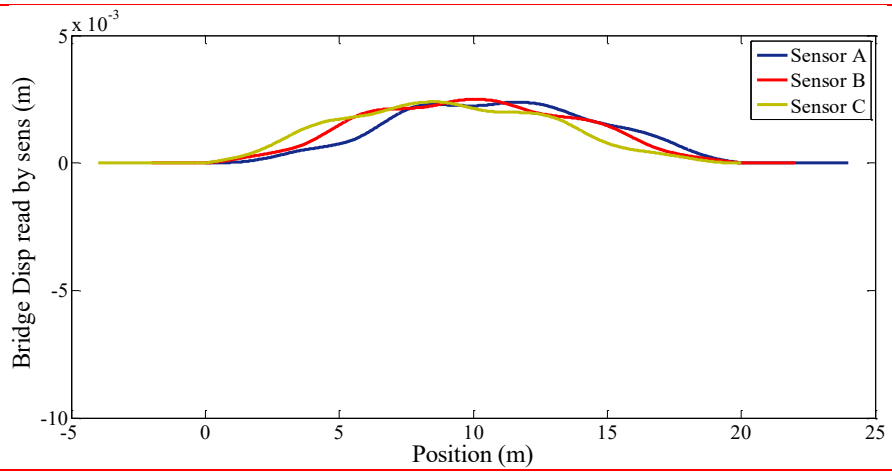

Fig. 5 The portion of the bridge displacements read by each of the sensors

For this typical example, the bridge displacements are considerably less than the bounce and pitch motions, and the road profile heights. A subtraction process, involving data read by each of the three sensors (Fig. 6), is proposed that will remove the influence of the bounce motions and contamination from the road profile.

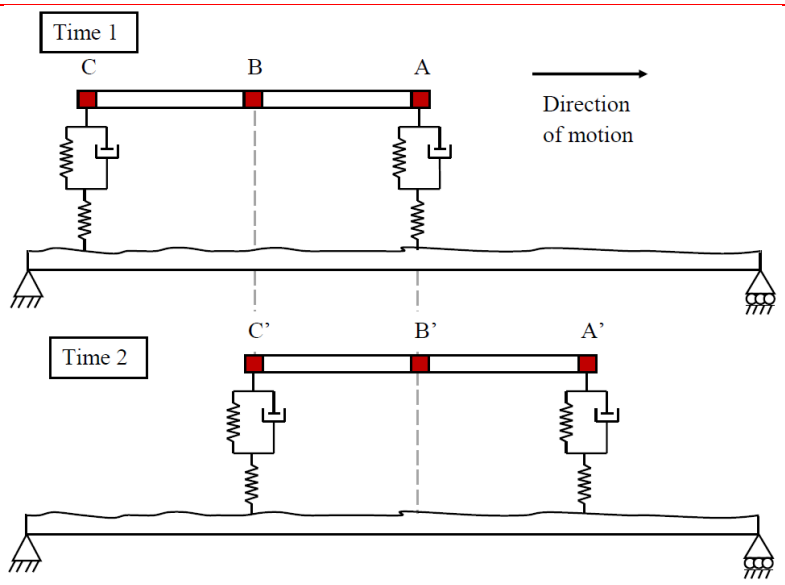

Fig. 6 The Traffic Speed Deflectometer (TSD) with three sensors

Initially, sensors A, B and C measure displacement at time t_1. At time t_2, sensor B reads displacement at the location of sensor A at time t_1 and sensor C reads displacement at the location of sensor B at time t_1. The monitoring time t_i is related to the speed of the vehicle and the location of the sensors. 'Time shifted curvatures' (Fig. 7) are found by subtracting data gathered from the three sensors:

$$Time-shifted\ \ Curvature=(h_A-h_B)-(h_B^{'}-h_C^{'}) \tag{11}$$

where $h_B^{'}$ is the displacement read by sensor B at t_2, which consists of bounce, pitch, $road_A$ and $bridge_B$ at t_2. $h_C^{'}$ is the displacement read by sensor C at t_2, which consists of bounce, pitch, $road_B$ and $bridge_C$ at t_2. The result of finding the time-shifted curvatures is that the profile heights and the bounce motions of the vehicle have been removed. Therefore the results are independent of the road profile presented in Figure 2. However, the time-shifted curvatures are still not sensitive to damage, as can be seen in Fig. 7. This is because the pitch motions of the vehicle are still present.

In the event of an acceleration or deceleration of the TSD, an adjustment will be made to ensure that the subtraction process continues to remove the influence of the road profile.

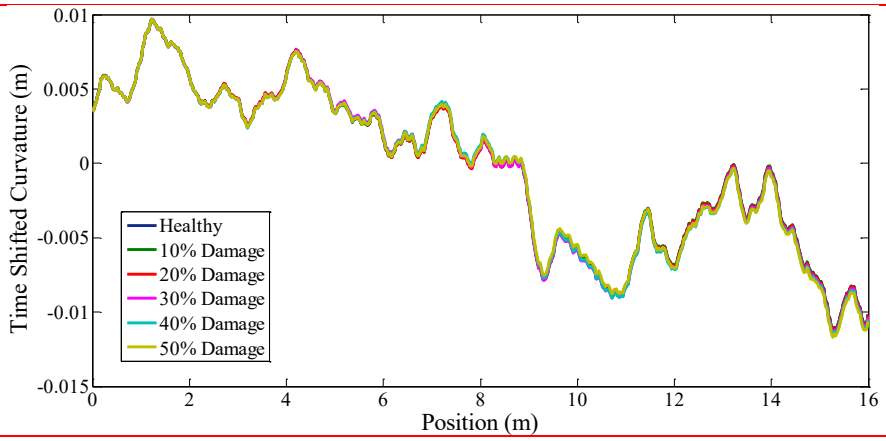

Fig. 7 The time-shifted curvature read by each of the sensors for different damage levels

4. Bridge damage detection using the TSD assuming the pitch is known

The simulations from the previous section are repeated here, assuming that the pitch can be measured accurately. This assumes a minimum of 5 sensors that can read to the nearest micron. Fig. 8 illustrates the time shifted curvature for five levels of damage, where the pitch motions have been measured, and removed.

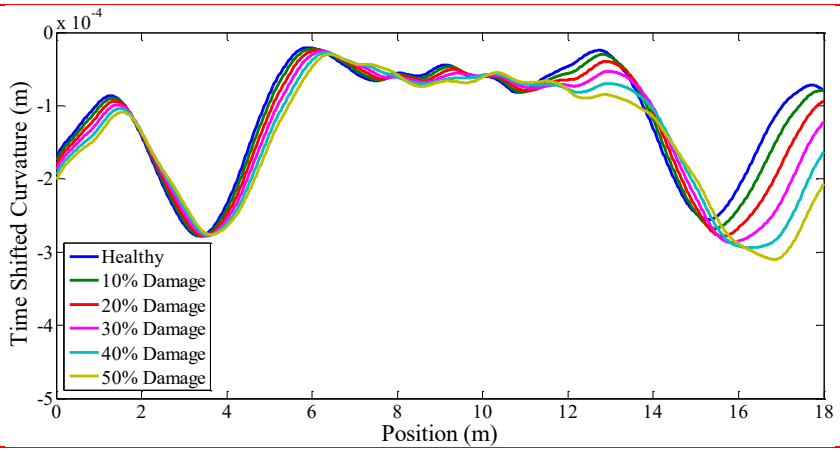

Fig. 8 Time-shifted curvatures, without pitch, read by each of the sensors for different damage levels

4.1 Varying transverse position and addition of noise

Thus far, the TSD has been simulated crossing the same single track of a randomly generated road profile. A carpet profile (Fig. 9) is generated from the initial road profile, correlating adjacent profiles transversely. The carpet profile generated has eleven alternative paths, and for each simulation, the path through the carpet is selected according to an assumed normal distribution for transverse location (Cebon and Newland, 1983).

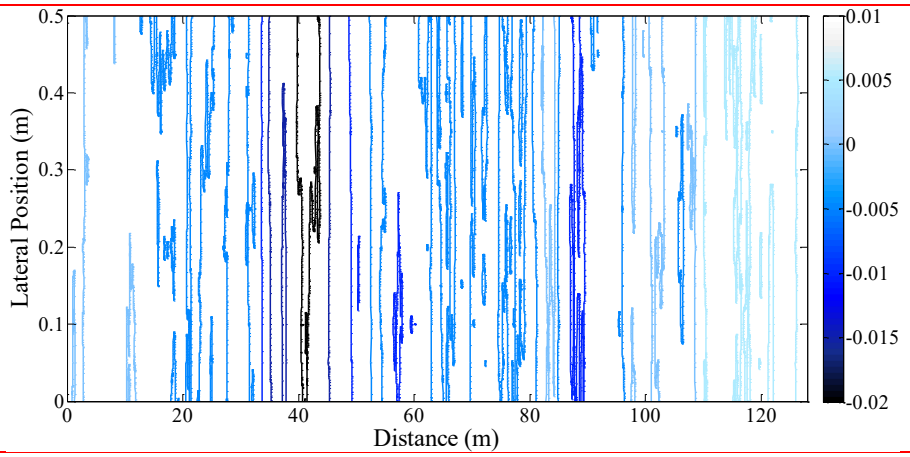

Fig. 9 Contours of level (m) for carpet profile

Additive White Gaussian Noise (AWGN), according to Lyons (2011), is added to the pitch measurements and to the displacements read by each sensor before the time shifted curvatures are calculated:

$$D_{poll} = D + E_{noise} * N \tag{12}$$

where D_{poll} is the signal containing noise, D is the original signal containing no noise, N is a standard normal distribution vector with zero mean and unit standard deviation and E_{noise} is the energy in the noise. The term, E_{noise}, is determined from the definition of the Signal to Noise Ratio (SNR) given by:

$$SNR = 10 \log_{10} \frac{\text{var}(D)}{E_{noise}^2} \tag{13}$$

which is the ratio of the power in the signal to the power in the noise and *var(D)* is the variance of the signal.

In these simulations, the SNR is specified, and $\text{var}(D)$ is easily determined. Using equation (13), noise at an SNR level of 75 is added to the beam displacements (which corresponds to noise of 5 microns). As before, the TSD traverses the bridge six times, once for the healthy case and once for each of the five damage levels. Each time the TSD crosses the bridge, it traverses a randomly selected path through the carpet profile and a different noise is added. The displacements are read by each of the three sensors, and the time-shifted curvatures are then determined (Fig. 10).

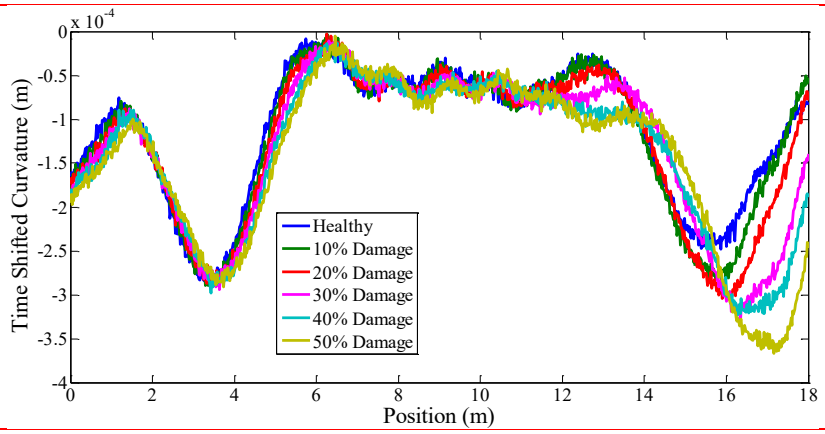

Fig. 10 Time-shifted curvature with noise

Fig. 10 shows the raw time-shifted curvature for different levels of damage. The raw signal (Fig. 10) is passed through a 9th order low pass Butterworth filter with a cut-off frequency of 20 Hz. The results of the filtering can be seen in Fig. 11.

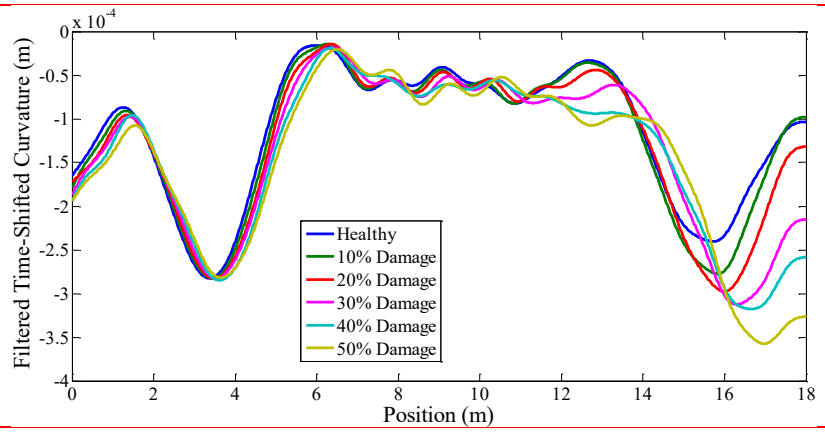

Fig. 11 The time-shifted curvature after filtering

This significantly improves the quality of the signal, giving a clear distinction between the different levels of damage. The RMS of the differences between time shifted curvature signals for different damage levels is investigated as a means of determining the repeatability of the approach. The TSD is simulated crossing the bridge fifteen times with varying transverse positions and noise signals. The RMS of the difference between a damage level and the healthy case is found (for each of the damage levels). These are plotted for each damage level and for each run and can be seen in Fig 12. The figure shows that, for an SNR of 75, the damage levels are distinct from one another and the approach is repeatable.

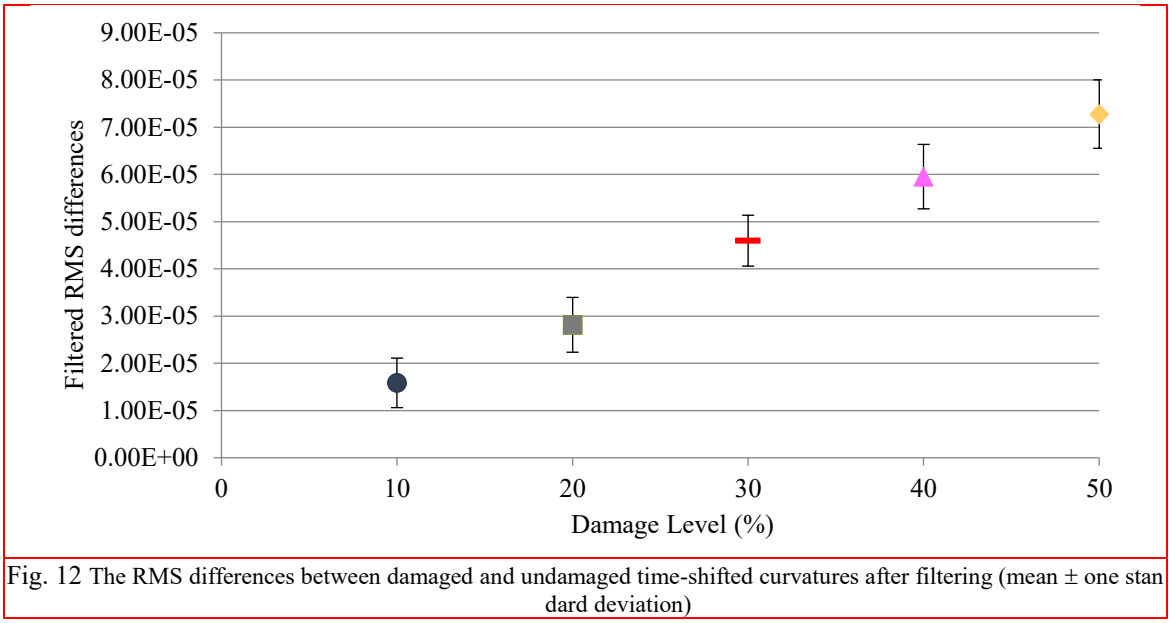

Fig. 12 The RMS differences between damaged and undamaged time-shifted curvatures after filtering (mean ± one standard deviation)

5. Bridge damage detection using the TSD with five sensors and time-shifted kurtosis

TSD's for pavement monitoring are not generally configured to remove pitch (Fig. 13). However, the current trend is towards TSD's with a greater number of sensors. If these sensors are sufficiently accurate (if they can read to the nearest micrometer), it is possible to remove the effects of pitch by calculating time-shifted kurtosis. Time-shifted kurtosis (Equation (14)) is tested here as a means of removing the influence of the pitch motions of the vehicle, as well as the bounce and road profile.

$$Time-shifted \quad Kurtosis=(h_A-2h_B+h_C)-(h_C^{'}-2h_D^{'}+h_E^{'}) \tag{14}$$

where h_A, h_B and h_C are the displacements read by sensors A, B and C at t_1, and $h_C^{'}$, $h_D^{'}$ and $h_E^{'}$ are the displacements read by sensors C, D and E at t_2.

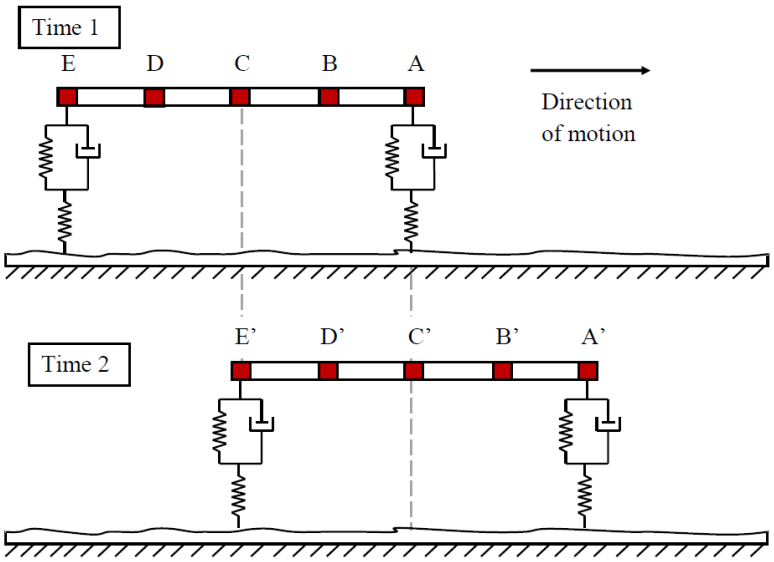

Fig. 13 TSD with five sensors

The bounce motions, pitch motions and the road profile drop out of the equation leaving only some component of bridge displacements. The TSD is simulated crossing a simply supported beam (with an approach length of 100 m which excites the vehicle initially) and with an ISO Class 'A' road profile. Damage is simulated as a loss in stiffness of one of the beam elements, in this case, the 14th element out of a total of 20 elements. Five different damage levels are simulated with 10%, 20%, 30%, 40% and 50% reduction in beam depth. The clear differences in the curves of Figure 14 show that time-shifted kurtosis is quite sensitive to damage.

Each time the TSD traverses the bridge on a randomly selected path from the carpet profile and a different noise is added. The displacements are read by each of the five sensors, and the time-shifted kurtosis is then determined. It is again passed through a 9th order low pass Butterworth filter with a cut-off frequency of 20 Hz and the results can be seen in Fig. 14. This significantly improves the quality of the signal giving a clear distinction between the different levels of damage.

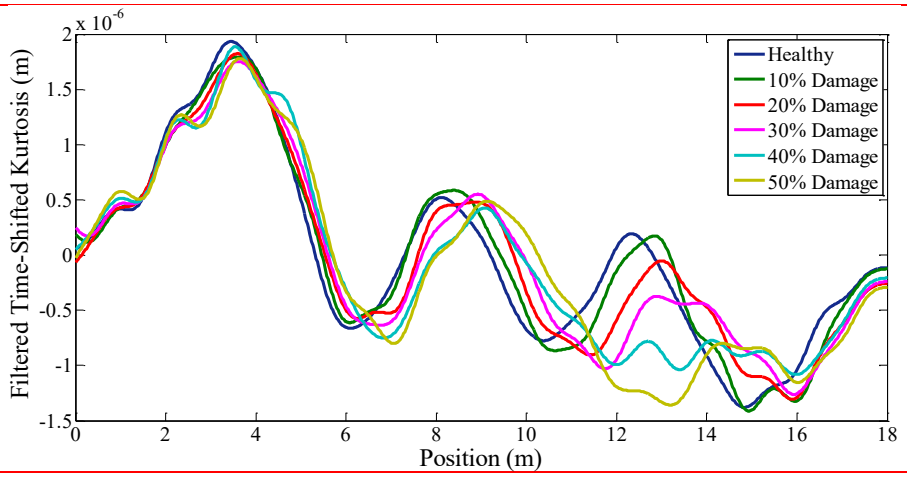

Fig. 14 Time-shifted kurtosis after filtering

The RMS of the differences between time shifted kurtosis signals for different damage levels is also investigated as a means of determining the repeatability of the approach. As before, the TSD traverses the bridge fifteen times with varying transverse positions and noise signals and the RMS of the difference between a damage level and the healthy case is found (Fig. 15). The figure shows that, for an SNR of 75, the damage levels are distinct from one another and the approach is repeatable.

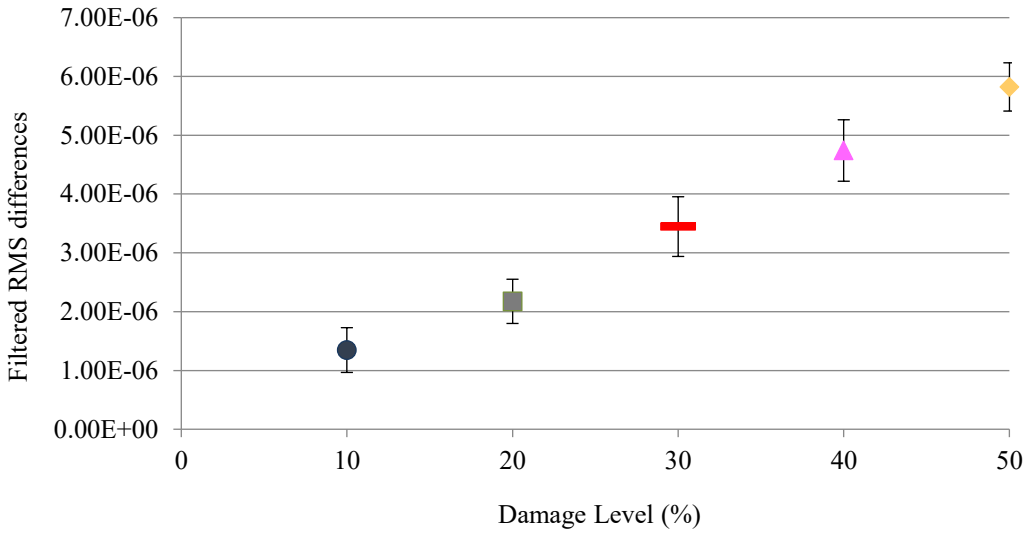

Fig. 15 The RMS differences between damaged and undamaged time-shifted kurtosis after filtering (mean ± one standard deviation)

A new variable, *Z*, is defined as the difference between one damage level and the next (say the difference between 10% and 20% damage). The probability is calculated of a failed diagnosis (= probability that $Z > 0$), i.e. the probability of an overlap in the cluster of points from two different

damage levels in Figure 15. Assuming the variables to be independent and Normally distributed, the probabilities of a failed diagnosis between each damage level are shown in Table 2, illustrating that there is a low probability of a failed diagnosis.

Table 2 Probability of a failed diagnosis

Damage Level	Probability
10% - 20%	0.0668
20% - 30%	0.00289
30% - 40%	0.00695
40% - 50%	0.01255

5. Conclusions

This paper investigates the feasibility of using a Traffic Speed Deflectometer to detect damage in bridges. The data gathered from the TSD is post-processed and time-shifted curvature, without pitch, is used as the damage indicator. These time-shifted curvatures, without pitch, remove the bounce motion of the vehicle, as well as contamination due to the road profile. Simulations show that, when pitch is measured, local losses of stiffness in a beam can be detected graphically using measurements from the TSD, even in the presence of realistic levels of noise (an SNR of 75). Simulations also reveal that the approach is insensitive to differences in the transverse position of the vehicle on the bridge from one measurement to the next. The paper then presents time-shifted kurtosis as a means of removing the pitch motions, as well as the influence of the road profile. If measurements are sufficiently accurate, damage can be detected graphically by examining a plot of the filtered time-shifted kurtosis against position.

It can be concluded that highly accurate displacement measurements taken from a traffic speed vehicle passing over a bridge, have the potential to detect damage at a point. However, it must be emphasised that the levels of damage being considered are substantial (even a 10% crack is a great deal of damage). While measurement noise has been considered, other sources of inaccuracy, such as wind, have not been. Further, changes in bridge behaviour due to environmental effects such as temperature may contaminate the damage indicator. Despite these shortcomings, the very high accuracy of existing TSD sensors, combined with the great advantages of a drive-by approach, means that this concept has good potential for bridge damage detection in the future.

Acknowledgments

The research described in this paper was financially supported by Science Foundation Ireland.

References

Bathe, K. J.; Wilson, E. L. 1976. *Numerical methods in finite element analysis*. Englewood Cliffs. New Jersey, NJ: Prentice-Hall.

Briggs, R. C.; Johnson, R. F.; Stubstad, R. N.; Pierce, L. 2000. A comparison of the rolling weight deflectometer with the falling weight deflectometer, In *Symposium on Nondestructive Testing of Pavements*

and Backcalculation of Moduli: Third Volume pp. 444–456. West Conshohocken, PA, USA.
Cebon, D. 1999. *Handbook of Vehicle-Road Interaction*. The Netherlands: Swets & Zeitlinger Lisse.
Cebon, D.; Newland, D. E. 1983. Artificial Generation of Road Surface Topography by the Inverse F.F.T. Method, *Vehicle System Dynamics*, ***12*(1-3)**, 160–165. DOI: 10.1080/00423118308968747.
Cerda, F.; Garrett, J.; Bielak, Barrera, J.; Zhuang, Z.; Chen, S.; Rizzo, P. 2012. Indirect structural health monitoring in bridges: scale experiments, In "*Bridge Maintenance, Safety, Management, Resiliance and Sustainability (IABMAS2012)"* pp. 346–353, Stresa, Italy: CRC Press, Taylor and Francis Group, London, UK.
Clough, R. W.; Penzien, J. 1975. *Dynamics of structures*. New York, NY: McGraw-Hill.
DAF Trucks Limited. (2012). *FAT CF75 30t Specification sheet*. Retrieved from http://www.atn.co.za/LinkWrap.asp?model_id=14091&filename=/specs/FATCF756X4RIGID%281%29.pdf&asset_name=D+A+F+FAT+CF75+Truck+Rigid.
González, A. 2010. Vehicle-bridge dynamic interaction using finite element modelling. In D. Moratal (Ed.), *Finite Element Analysis* pp. 637–662.
González, A.; Covián, E.; Madera, J. (2008). Determination of bridge natural frequencies using a moving vehicle instrumented with accelerometers and a geographical positioning system, In *Proc of the 9th International Conference "Computational Structures Technology",* Athens, Greece.
González, A.; Hester, D. 2013. An investigation into the acceleration response of a damaged beam-type structure to a moving force, *Journal of Sound and Vibration*, **332(13)**, 3201–3217. DOI: 10.1016/j.jsv.2013.01.024
González, A.; OBrien, E. J.; McGetrick, P. J. 2012. Identification of damping in a bridge using a moving instrumented vehicle, *Journal of Sound and Vibration*, **331(18)**, 4115–4131. DOI: 10.1016/j.jsv.2012.04.019
Hester, D.; González, A.; Rowley, C. W. 2008. Examining the dynamic response of a deteriorated due to the passagfe of moving loads, In *Procs of the Bridge and Concrete Research in Ireland Conference,* Galway, Ireland.
Harris, N. K.; OBrien, E. J.; González, A. 2007. Reduction of bridge dynamic amplification through adjustment of vehicle suspension damping, *Journal of Sound and Vibration*, **302(3)**, 471–485. DOI: 10.1016/j.jsv.2006.11.020
Jenkins, M. 2009. Geometric and Absolute Calibration of the English Highways Agency Traffic Speed Deflectometer, In *Young Researchers Seminar*, p. Session 6, paper 3, Torino, Italy.
Keenahan, J.; OBrien, E. J.; McGetrick, P. J.; González, A. 2014. The use of a dynamic truck-trailer drive-by system to monitor bridge damping, *Structural Health Monitoring* **13(2)** 183-197.
Kim, C.W., Chang, K.C., Kitauchi, S. & McGetrick, P.J. 2016. A field experiment on a steel Gerber-truss bridge for damage detection utilizing vehicle-induced vibrations, *Structural health monitoring*, **15:** 174-192.
Kim, C.W., Chang, K.C., McGetrick, P.J., Inoue, S. & Hasegawa, S. 2017. Utilizing moving vehicles as sensors for bridge condition screening—a laboratory verification, *Sensors and Materials*, **29**, 153-163.
Kim, C.W.; Kawatani, M. 2009. Challenge for a drive-by bridge inspection, In *Procs of the 10th International Conference "Structural Safety and Reliability, ICOSSAR2009"* pp. 758–765, Osaka, Japan: CRC Press, Taylor and Francis Group, London, UK.
Lin, C.W.; Yang, Y. B. 2005. Use of a passing vehicle to scan the fundamental bridge frequencies: An experimental verification, *Engineering Structures*, **27(13)**, 1865–1878. DOI: 10.1016/j.engstruct.2005.06.016
Lyons, R. G. 2011. *Understanding Digital Signal Processing,* Boston, MA: Prentice-Hall.
McGetrick, P J; Kim, C. W.; O'Brien, E. J. 2010a. Experimental Investigation of the Detection of Bridge Dynamic Parameters using a Moving Vehicle, In *The Twenty-Third KKCNN Symposium on Civil Engineering*. Taipei.
McGetrick, P.J.; González, A.; O'Brien, E. 2010b. Monitoring bridge dynamic behaviour using an instrumented two axle vehicle, In *Bridge and Concrete Research in Ireland*. Cork, Ireland.
McGetrick, P.J.; González, A.; OBrien, E. J. 2009. Theoretical investigation of the use of a moving vehicle to

identify bridge dynamic parameters, *Insight: Non-Destructive Testing & Condition Monitoring*, ***51***, 433–438. DOI: no

McGetrick, P.J., Hester, D. & Taylor, S. 2017. Implementation of a drive-by monitoring system for transport infrastructure utilising smartphone technology and GNSS, *Journal of Civil Structural Health Monitoring*, **7**, 175-189.

McGetrick, P.J., Kim, C.W., Gonzalez, A. & OBrien, E.J. 2015. Experimental validation of a drive-by stiffness identification method for bridge monitoring, *Structural Health Monitoring*, **14**, 317-331.

McGetrick, P.J.; Kim, C. W.; González, A.; OBrien, E. J. 2013. Dynamic axle force and road profile identification using a moving vehicle. *International Journal of Architecture, Engineering and Construction*, **2(1)**, 1–16.

OBrien, E.J., Martinez, D., Malekjafarian, A. & Sevillano, E. 2017. Damage detection using curvatures obtained from vehicle measurements, *Journal of Civil Structural Health Monitoring,* **7,** 333-341.

Oshima, Y.; Yamaguchi, T.; Kobayashi, Y.; Sugiura, K. 2008. Eigenfrequency estimation for bridges using the response of a passing vehicle with excitation system, In *Proc of the 4th International Conference "Bridge Maintenance, Safety and Management, IABMAS2008",* pp. 3030–3037, Seoul, Korea: CRC Press, Taylor and Francis Group, London, UK.

Sinha, J. K.; Friswell, M. I.; Edwards, S. 2002. Simplified Models for the Location of Cracks in Beam Structures Using Measured Vibration Data, *Journal of Sound and Vibration*, **251(1)**, 13–38. DOI: 10.1006/jsvi.2001.3978

Tedesco, J. W.; McDougal, W. G.; Ross, C. A. 1999. *Structural dynamics: theory and applications*. California, CA: Addison Wesley Longman.

Toshinami, T.; Kawatani, M.; Kim, C. W. 2010. Feasibility investigation for identifying bridge's fundamental frequencies from vehicle vibrations, In *Proc of the 5th International Conference "Bridge Maintenance, Safety and Management IABMAS2010"* pp. 317–322, USA: CRC Press, Taylor and Francis Group, London, UK.

Weaver, W.; Johnston, P. R. 1987. *Structural dynamics by finite elements*. Indiana: Prentice-Hall.

Yabe, A.; Miyamoto, A. 2012. Bridge condition assessment for short and medium span bridges by vibration responses of city bus, In *Proc of the 6th International Conference "Bridge Maintenance and Safety"*, July, 2012, Stresa, Italy, pp. 195-202.

Yang, Y. B.; Chang, K. C. 2009. Extraction of bridge frequencies from the dynamic response of a passing vehicle enhanced by the EMD technique, *Journal of Sound and Vibration*, **322(4-5)**, 718–739. DOI: 10.1016/j.jsv.2008.11.028

Yang, Y. B.; Li, Y. C.; Change, K. C. 2012. Using two connected vehicles to measure the frequencies of bridges with rough surface: a theoretical study, *Acta Mechanica*, *223*(8), 1851–1861. DOI: no

Yang, Y. B.; Lin, C. W.; Yau, J. D. 2004. Extracting bridge frequencies from the dynamic response of a passing vehicle, *Journal of Sound and Vibration*, **272(3-5)**: 471–493. DOI: 10.1016/S0022-460X(03)00378-X

Yang, Y. B.; Yau, J. D.; Wu, Y. S. 2004. *Vehicle-Bridge Interaction Dynamics: with Applications to High-Speed Railways*. Singapore: World Scientific Publishing Co. Ltd.

Some of the conference papers listed about are available at UCD's Research Repository at: http://researchrepository.ucd.ie/